Conference paper

Pavel N. Nesterenko*

3D printing in analytical chemistry: current state and future

https://doi.org/10.1515/pac-2020-0206

Abstract: The rapid development of additive technologies in recent years is accompanied by their intensive introduction into various fields of science and related technologies, including analytical chemistry. The use of 3D printing in analytical instrumentation, in particular, for making prototypes of new equipment and manufacturing parts having complex internal spatial configuration, has been proved as exceptionally effective. Additional opportunities for the widespread introduction of 3D printing technologies are associated with the development of new optically transparent, current- and thermo-conductive materials, various composite materials with desired properties, as well as possibilities for printing with the simultaneous combination of several materials in one product. This review will focus on the application of 3D printing for production of new advanced analytical devices, such as compact chromatographic columns for high performance liquid chromatography, flow reactors and flow cells for detectors, devices for passive concentration of toxic compounds and various integrated devices that allow significant improvements in chemical analysis. A special attention is paid to the complexity and functionality of 3D-printed devices.

Keywords: analytical chemistry; 3D printing; Mendeleev-21; reactors; separation; sensors.

Introduction

There are no doubts that additive technologies, in particular 3D printing, are making remarkable changes in various fields of science and technology including chemistry [1]. The possibility to make accurate and reproducible prototypes of devices having very complex, sometimes unique, geometry in a short time, simplicity of modification and improvements of 3D design of printed objects by simple changes in computers files associated with the original model, simultaneous multi-material printing, low cost of major types of 3D printers and supplies for them along with many others advantages make 3D printing as extremely useful and popular technology in chemical laboratories. In the last decade 3D printing provided a significant breakthrough in construction and production of various tools, instrumental parts and devices for various applications in analytical chemistry [2]. There are several published reviews on use of 3D printing in the relevant areas including separation sciences [3, 4], optical sensing and biosensing [5–8] and microfluidics sensing [9].

The aim of this critical review is not to provide exhaustive description of all 3D printed objects and details of their exploitation in analytical chemistry, but to analyse possibilities for printing objects of elevated geometric complexity, unusual design and complex material functionality, which resulted in substantial improvements of established methods of chemical analysis or ingenious solutions for opening new possibilities in the development of new analytical methods. The corresponding classification of the 3D printed objects is proposed.

Article note: A collection of invited papers based on presentations at 21st Mendeleev Congress on General and Applied Chemistry (Mendeleev-21), held in Saint Petersburg, Russian Federation, 9–13 September 2019.

^{*}Corresponding author: Pavel N. Nesterenko, Department of Chemistry, Lomonosov Moscow State University, 1–3 Leninskie Gory, GSP-3, Moscow, Russian Federation, e-mail: p.nesterenko@phys.chem.msu.ru

Four levels of functionality of 3D printed devices and auxillary tools

The most important characteristics of 3D printed objects include their geometry and spatial structure, which must fulfil the required operational needs and provide maximal efficiency and operational convenience of constructed analytical device. In terms of complexity and production difficulty 3D printed objects can be divided in two types. The first type has open space geometry with an easy access to holes, channel and cavities, when the use of supporting material is not required during printing or, if used, this material can be easily removed/washed out to obtained clean final product. The second type of the objects has closed or almost closed space geometry with many functional volumes located inside of printed body and linked with outer space through narrow channels and capillaries. Obviously, the removal of supporting material, e.g. poly(acryloylmorpholine) polymer (SUP707 material, Stratasys, VIC, Australia) commonly used in photopolymerisation 3D Polyjet printing mode, from narrow long channels and small cavities can represent a serious problem due to slow dissolution of polymer and slow diffusion of dissolved polymer to the open end of the channel. It was found that the complete washing of poly(acryloylmorpholine) out of printed flow cell having spiral configuration with 64 mm long and 1 mm internal diameter requires 360 h [10].

Further, based on geometry and functionality of 3D printed materials the analytical devices can be divided in four groups (Table 1). The first group joined simple open geometry devices, which include various holders, housings, joints, simple tools etc. The properties of materials may have insignificant role, when the ability of the material to keep the shape of printed object is the only requirement for this group. The second group has functional closed geometry volumes and channels. The properties of materials are still not too important with only requirement to keep mechanical stability in contact with liquid phase passing through internal volumes and channels. The next group joins devices where physico-chemical properties play an important role for the correct functioning of printed parts. It could be elevated mechanical strength, electrical and thermal conductivity, magnetic properties, light transmittance and others. Finally, the last group includes analytical devices with a significant impact of chemical properties of the internal surface and heterophase reactivity of the printed materials in their functioning. In this case heterophase reactivity means the presence of specific adsorption properties of 3D printed materials or specifically attuned adsorption, catalytic and sensor activity achieved by additional chemical modification of their surface. Some of combinations such as open space devices with chemical functionally of the surface of printed material are not included in the table. Usually this option is referred to printed electrodes or thin layered sensors having rather 2D geometry configuration.

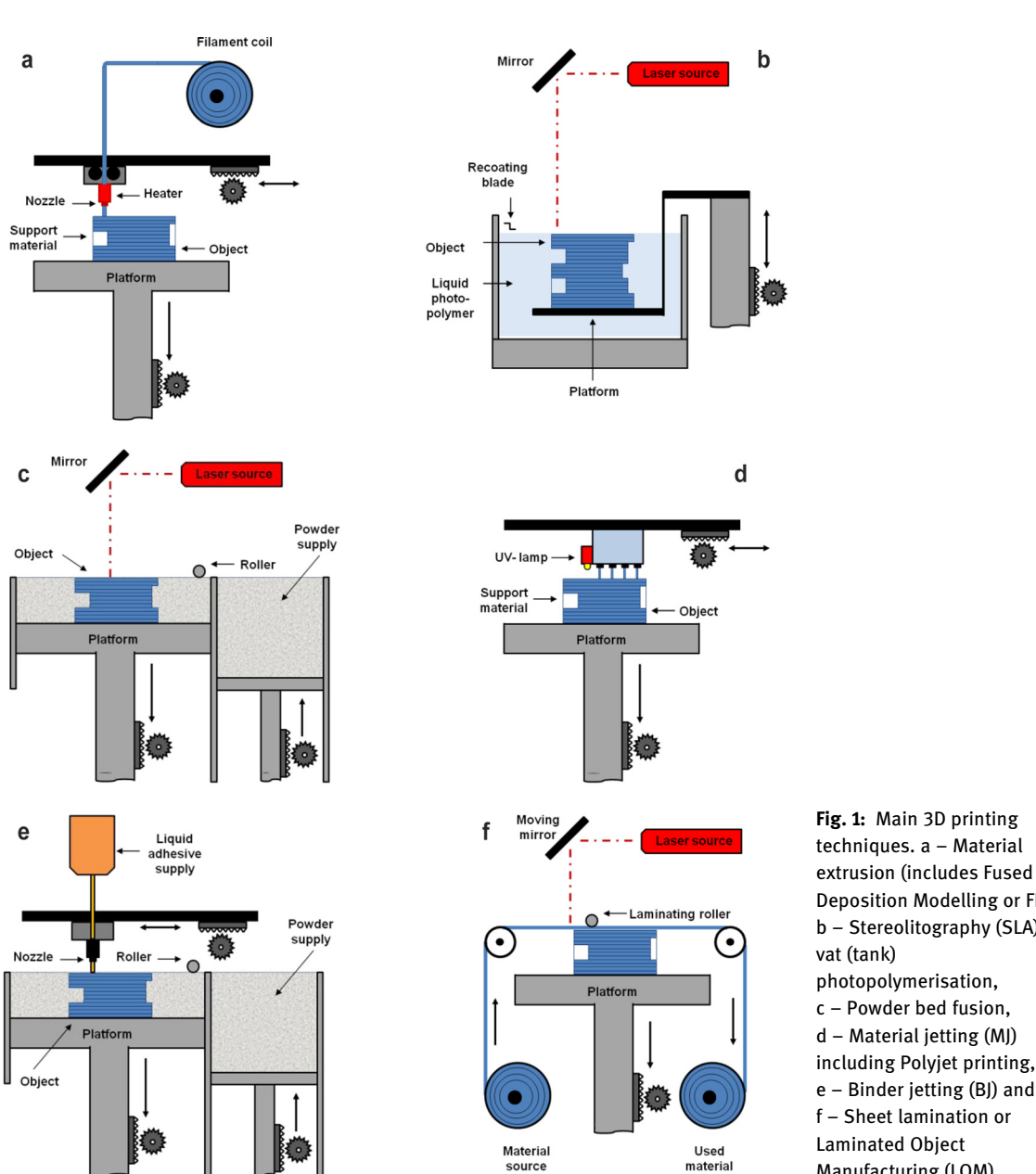
3D Printing techniques

The key 3D printing techniques are schematically shown in Fig. 1. The main difference between techniques is connected with build material delivery and its solidification for constructing of 3D object. Printing material can be delivered in a liquid form by extrusion of fused polymer (e.g., Fused Deposition Mode or FDM, Fig. 1a), by

Table 1: Classification of 3D printed device used in analytical chemistry according to their complexity and functionality.

Group Geometry		Functionality of printed material			
1	Open space	Insignificant with minimal requirements to mechanical stability.			
2	Closed space with complex internal structure	Defined by the internal structure, the role of material is not significant except of mechanical stability.			
3	Closed space with complex internal structure	Based on specific physico-chemical properties such as elevated mechanical stability, electric and thermal conductivity, magnetic, optical transparency and others. These properties of the build material can be modified by addition of solid particles.			
4	Closed space with complex internal structure	Surface chemistry plays an important role, internal surface of objects can be additionally modified. The objects may include embedded particles for modification of chemical properties.			

mechanical coating a top of printed object with thin liquid layer of photosensitive polymer (e. g. stereolithography or SLA, Fig. 1b) and by formation of thin liquid layer by spraying of photosensitive polymer on a top of printed object (e. g. material jetting including Polyjet printing, Fig. 1d). A simple hardening of melted polymer during cooling (FDM) and photopolymerisation (SLA, Polyjet printing) provides the final formation of 3D object. The geometrical configuration of 3D printed object is controlled by computer with either target delivery (FDM, Polyiet printing) or precize photopolymerization of liquid supply material (e. g. mask based laser writing) within the loaded layer according to the selected model (SLA). In some cases additional curing of photopolymerised material is required. Obviously, the use of liquids has advantage in terms of homogeneity of printed material, simplicity of changing resulting properties of the objects by simple modification of the composition in liquid supply, lower printing resolution and simplified possibility of multi-material printing. Typical layer resolution and accuracy down to 14 µm is characteristic for Polyjet printing technique. The best reported printing resolution is between 10 and 20 μm for FDM and 18–25 μm for SLA, respectively [1].



Deposition Modelling or FDM), b - Stereolitography (SLA) or vat (tank) photopolymerisation, c – Powder bed fusion, d - Material jetting (MJ) including Polyjet printing, e - Binder jetting (BJ) and f - Sheet lamination or Laminated Object Manufacturing (LOM).

Microparticle powders of polymer, metal and various inorganic substances are normally used as solid supply materials in power bed fusion technique (Selective Laser Sintering or SLS, Selective Laser Melting or SLM, Fig. 1c), binder jetting technique also known as Inkjet printing (Fig. 1e), while polymer or metal sheets are used in sheet lamination technique (Fig. 1f) including ultrasonic additive manufacturing (UAM). In power bed fusion the printing process includes formation of thin layers of microparticles followed by laser sintering or melting. For binder jetting techniques the addition of binding component is required followed by special chemical reactions, photopolymerisation or thermally induced process resulting in binding of microparticles according to the computer model. Thin sheets or films of polymers and foils of metals represent build material in sheet lamination technology based on "bond-then-form" principle. One of the promising options in sheet lamination technology is ultrasonic metal welding (USW) process, which differs substantially from other welding processes due to consolidation of solid materials at temperatures far below their melting points [11]. Of course, laser melting is also used in sheet lamination. 3D printing methods based on using solid microparticles as build material have a limitation on printing resolution, which depends strongly on particle size and distribution of particles on size. Obviously, the maximum resolution cannot be less than diameter of particles used. Usually, 40–100 µm particles are normally used in SLS and SLM and therefore printing resolution is limited by upper limit of size distribution. but a lower layer resolution of 25 µm has been reported by using fine metal particles [12].

Another important aspect is the cost of 3D printers and 3D printing supplies. As a rule the cost of 3D printers using nonparticulate build material (e.g., low melting polymer filament in FDM, liquid photopolymer in SLA) are significantly cheaper than of printers using particulated build material (powder in SLS, microdrops of sprayed phopolymer in Polylet printing). The average cost of FDM and SLA printers is about 1000 USD and 5000 USD, respectively [1]. For comparison, the cost of SLS printer is approximately 10,000 USD for printing plastic and 70,000700,000 USD for printing titanium powders. It should be noted that the cost of titanium aluminium-vanadium alloy Ti6Al4V particles, common for 3D printing of metal objects, is approximately 500 USD/kgfor spherical particles of diameter between 15 and 53 µm. The same cost is reported for 80 nm particles of stainless steel, which is another popular material for SLS printing technique.

It should be noted that consumption of solid particles in solid phase 3D printers is quite high as particles play also a role of support material during printing as shown in Fig. 1c, and 1e. At the same time, 1 kg of filament of poly(lactic acid) or PLA, one of the most popular material for FDM printing technique, can be purchased for 5–7 USD. Undoubtedly, the cost of printing depends strongly on printing resolution and it may be extremely high. The cost of another type of 3D printers using particles and known under general name Material jetting is between 50,000 and 250,000 USD.

The terminology and classification of various options in 3D printing technologies is not well established and has resulted in various names, often attributed to different trade names, given to similar methods. For example, powder bed fusion technology includes not only SLS and SLM (also known as Direct Metal Laser Sintering (DMLS)) methods, but also Electron Beam Melting (EBM) and Multi Jet Fusion (MJF) methods. This technology overlaps significantly with LENS, Aerosol Jet, Electron Beam Additive Manufacturing (EBAM) and Laser Deposition Welding (LDW) techniques positioned under umbrella of Directed Energy Deposition (DED) 3D printing technology. Simirlarly, photopolymerisation 3D printing technology includes Digital Light Processing (DLP), Continuous Liquid Interface Production (CLIP) and Daylight Polymer Printing (DPP) along with well-known SLA. The big number of different names results in some confusion of final users of 3D printed products, which may expect a substantial difference in their properties. Fortunately, this is not fatal and different 3D printing techniques can be used for the printing/production of the same product as can be concluded from the application of 3D printed devices in chemistry. However, the detailed consideration of various 3D printing techniques is not included in this review.

General areas of 3D Printing applications related to chemistry

The widespread use of 3D printed objects in chemistry is defined by few factors. A key reason is associated with the possibility of production of devices with very complex geometry. This is extremely useful for the construction of analytical instrument components, sophisticated flow reactors, separators, scavengers, flow cells and other parts allowing sequence of manipulations with target substances in a flow mode. The second reason is connected with a diversity of materials, which can be printed. The major materials used in 3D printing technologies are organic polymers, which can possess many useful properties such as biocompatibility, optical transparency, thermal and electric conductivity and others [13]. Moreover, the development of new polymer based composite materials with added fillers makes possible to improve selectivity of heterophase reactions and attune physico-chemical properties of build materials in 3D printing. Therefore, the option of multi-material 3D printing provides unique possibilities for the production of sophisticated devices combining various functions such as preconcentration, mixing, selective reactions, separation and detection in one compact piece of instrumentation. Undoubtedly, an intensive introduction of 3D printing in chemical research practise has opened a new era in the development of microfluidics and portable analytical instrumentation. So, according to research papers on application of 3D printing technologies in chemistry about 51% works are associated with analytical chemistry (see Fig. 2, left). Surprisingly, 13% of applications are related to pharmaceutical chemistry with focus on drug delivery options. The possibility of simple production of complex 3D objects is frequently used in education with 6% impact to whole number of applications. Undoubtedly, the use of three dimensional complex chemical structures provides better and faster understanding of group symmetry in crystallochemistry, macromolecules configuration in biochemistry, optical isomerism in stereochemistry and in many other fields of chemistry. Finally, good biocompatibility of some organic polymers determines application of 3D printed devices for conducting of various bioassays, cells sorting, electroporation and drug testing in biochemistry with 5% of total applications. A superior chemical and mechanical stability is required for chemical reactors designed for the use of aggressive reagents, so powder bed fusion of titanium alloys and stainless steel particles can be used for their production. A relatively high cost of metal printing resulted in only 3% contribution of synthetic chemistry applications. By considering that many applications such as bioassays and polymerase chain reactors in biochemistry and drug screening in pharmaceutical chemistry are also related to analytical chemistry the total part of applications of 3D printing technologies in this discipline can reach 75–80% of total number of applications.

The distribution of usage of different 3D printing techniques in analytical chemistry is shown in Fig. 2, right. Clearly, the cost of printer and supply materials is a decisive factor in selection of the technique with material extrusion and photopolymerisation covering more than 70% of practical needs. In some papers the comparison of two or three 3D printing techniques is reported for production of the same device. For example, material extrusion (FDM), photopolymerisation (SLA) and material jetting (Polyjet printing) techniques were compared for the fabrication of microfluidic device in terms of minimal possible size of channels, roughness of the printed surface and cost of production [14].

There are numerous applications of 3D printing technologies in analytical chemistry, which are summarised in recently published monograph [1] and reviews [2, 15]. Many more reviews have been also published on more specific topics including applications of 3D printing in organic synthesis [16, 17], catalysis [18–20], microfluidics [21], separation science [3], electrochemistry [22] and for printing labware [23]. However, the present review is about use of 3D printing technology in analytical chemistry with emphasis on various levels of complexity and functionality of printed objects.

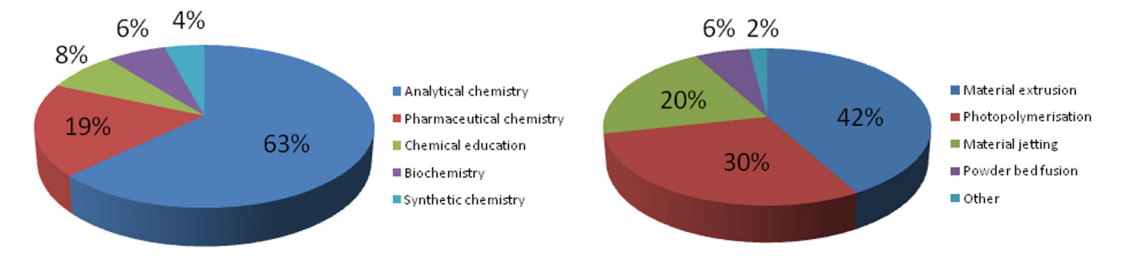


Fig. 2: Application of 3D printing in different disciplines of chemistry (left) and different 3D printing techniques in analytical chemistry (right).

Level 1: 3D printing of objects with useful open space geometry and indifferent role of printed material

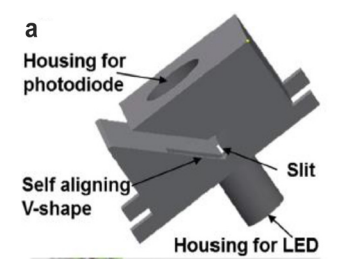
There is always a strong demand in the analytical laboratory for 3D printing of certain objects having non-standard shape and size but useful geometry. The primary functions of these objects include holding and housing of something simple and useful like ampoules, test tubes, lamps, centrifuge inlays, small spare parts etc. Obviously, in this case the requirements to precision and resolution of 3D printing are not too high and simple low cost FDM printer using cheap PLA, acrylonitrile butadiene styrene (ABS) or polypropylene plastics may fulfil all requirements including sufficient mechanical stability properties. The nice overview of simple 3D printed labware (also called Open Labware) is given by Baden [23]. Importantly, computer files of the corresponding models for 3D printing can be found in Internet library (e. g. https://www.thingiverse.com) and used directly by beginners in any other laboratory. A list of relatively simple, but useful for analytical laboratory devices, includes parts and components of magnetic stirrer, syringe pump, water bath, optical microscope, micropipette, hot plate, micromanipulator and other laboratory equipment.

Nevertheless, rather complex constructions can be produced in this category of 3D printed objects. For example, Cecil et al. used FDM mode of 3D printing for production of on-capillary spectrophotometric detector body [24]. The detector body printed with black PLA and had complex open space geometry as shown in Fig. 3 with six functional parts. They included housing for blue light emitting diode (LED) as light source, another housing for silicon photodiode detecting transmitted light, capillary self-aligning insertion slot ending with V-shape holder and a lever for tight keeping capillary relatively light beam slit, and two holes for fixing of detector body in capillary electrophoresis (CE) or flow-injection analysis (FIA) instruments. Slit dimensions of $50-900~\mu m$ (width \times length) are successfully printed for CE detector using fused silica capillaries of outer diameter (o.d.) $360~\mu m$ and internal diameter (i.d.) 50, 75 and $100~\mu m$ and for FIA experiments with fluorinated ethylene propylene tubing with an i.d. of $200~and~500~\mu m$ and o.d. $1000~and~1500~\mu m$, respectively. The performance of the 3D printed detector housing was comparable with a commercially available interface using the CE separation of zinc and copper complexes with [4 – (2-pyridylazo)-resorcinol] or PAR. The developed method was applied for the determination of these metals in river water.

It should be noted that Level 1 complexity 3D printing for the production of various parts of detector's bodies having no contacts with analyte flow is quite useful and cost effective. Recently, this approach has been used for preparation of complex components for a miniature LED-induced fluorescence detector for CE [25, 26], thermostates for CE cartridges improving mass-spectrometric (MS) and capacitively coupled contactless conductivity (C4D) detectors [27].

Level 2: 3D printed devices with complex internal geometry and insignificant role of the build material: key focus on internal lines

The devices under this level of complexity differ from above considered group of 3D printed objects by more sophisticated geometry of internal volumes and connections, which are rather closed. This means that additional attention should be attributed to more careful selection of support material for 3D printing of the relevant structures. The resolution of 3D printers is also of great importance in this case to achieve an acceptable roughness of internal walls, which can be influence the flow profiles of liquids, especially, in narrow channels and mixing points. However, the interaction between solutes from liquid or gas phases and solid build material of internal walls of printed objects is minimal or non-significant for the operational needs



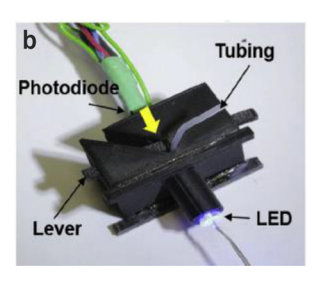


Fig. 3: Multifunctional 3D printed on-capillary detector body with integrated slit. Adapted from [24].

in this group of devices. Simply, the build material should have sufficient mechanical and chemical stability to manipulate with liquids under static and dynamic conditions [28]. Correspondingly, the most common 3D printed devices under Level 2 complexity include various mixers, flow reactors, droplet generators, switching and injection valves and housing for reactive (non-printed) elements like cartridges packed with selective adsorbents, porous filters and membranes, electrodes, coolers etc.

The representative examples of these devices designed for fluidics applications are listed in Table 2. Obviously, these fluidics devices can be used in various combinations for assays and as a part of more complex instruments as FIA analysers and gel electrophoresis apparatuses. For example, FIA system designed for determination of heavy metal ions natural waters contains 3D printed holder for SPE cartridge, reagent mixer and flow reactor connected in series in a single unit [33, 34].

The unique possibility of 3D printing for production of complex internal geometry was clearly demonstrated in work on influence of 3D configuration of 30 cm long capillary channel on chromatographic performance of separation columns [12]. By using SLM technique the authors printed titanium chromatographic columns having 2D spiral, 3D spiral and 3D serpentine types of channels as shown in Fig. 4a-c. Then internal walls were filled with organic polymer monolith according to [42] and peak broadening or column efficiency of the prepared columns was tested.

Obviously, the distance, which analyte molecules passed in chromatographic column, depends on channel curvature. Therefore, this results in distortion of the axial velocity profile and effects on chromatographic peak broadening/column efficiency. Theoretically, a minimal peak broadening should be expected for 3D serpentine configuration providing same migration distance for all analyte molecules injected as a plug of liquid solution at the top of corresponding chromatographic column. The chromatograms shown in Fig. 4d clearly demonstrated a significant advantage of 3D serpentine column over two other configurations. It should be underlined here that the production of titanium columns having such complex configurations would be practically impossible without application of 3D printing technology.

An impressive example of similar type of research has been reported by Dimartino et al. [32], who used 3D printing for production of chromatographic porous monolithic beds having structural units of different configuration such as truncated icosahedral (pseudo spherical), tetrahedral, octahedral, triangular bipyramidal and stellar octangular. The comparison of produced monoliths showed the efficiency for face-centred cubic (minimum plate height $H_{min} = 0.65$) and body-centred cubic ($H_{min} = 0.89$) pseudo spherical structural units, which are similar to tight packing of spherical particles into chromatographic column. Surprisingly, very good efficiency (H_{min} = 0.90) was obtained for tetrahedral structural units that provides strong evidence regarding possibility of getting highly efficient separations on chromatographic columns packed with nonspherical particles. There are other studies of this research group on structural effects of 3D printed stationary phases for liquid chromatography [32, 43, 44]. The considered results were obtained for non-retained analytes, so there are no specific interactions with printed objects in these chromatographic systems. For this reason these 3D printed devices are included in Level 2 functional complexity devices.

Level 3: 3D printed devices with functional internal volumes and cavities with a significant role of physicochemical properties of build material.

As noted the role of build material for 3D printed devices described in two previous sections was not too important for their operation. However, a growing attention has been revealed to the use of specific physicochemical properties to expand the functional possibilities of printed objects. Therefore, the next level of functional complexity of 3D printed devices for the use in analytical chemistry has to be associated with combination of complex geometry of objects and specific physico-chemical properties of special organic polymers or composite materials. The corresponding opportunities for possible applications are summarised in Table 3.

The advantages of combination of complex internal geometry of flow cell for chemiluminescent detector and optical transparency of build material was demonstrated in work [10]. Standard configuration of flow cell used for chemiluminescent detection is simply coiled narrow polymeric or glass tubing. However, the formation of the flat spiral flow cell from rigid tubing is rather difficult and irreproducible. Extra flexibility in flow cell design and complexity as well as improved reproducibility can be achieved by using expensive and time

Table 2: 3D printed fluidic devices and their components with complex internal geometry with insignificant interactions of build material with analytes.

Devices	Printing		Application	Ref.
	Material	mode		
Injection valve			ICP-MS online monitoring of extracellular Ca ²⁺ and Zn ²⁺ in living rat brains	[29]
Knotted type flow reactor	PA	SLA	Quantitative assessment of Ag ⁺ ions and AgNPs in municipal wastewater	[30]
Cyclonic spray chamber for ICP-OES	ABS/PLA	FDM	Possibility of using in ICP related applications for detection of metals	[31]
Chromatographic columns	Titanium alloy (Ti6Al4V)	SLM	Investigating the effect of column geometry on separation efficiency on separation of proteins	[12]
	ABS	MJ	3D printed porous beds with different unit shapes to investigate effects of mass transfer on column efficiency	[32]
FIA unit (SPE cartridge holder, mixer and flow	PMMA	SLA	Determination of Pb in river waters using preconcentration on TrisKem Pb resin followed by photometric detection with PAR	[33]
reactor)	PA	DLP	Determination of Cd and Pb in river waters using preconcentration/ separation on TrisKem Pb and Amberlyte 120 resins followed by fluorimetric detection with Rhod-5N	[34]
FIA unit (microcube mixers and SPE cartridge holder)	PMA based	SLA	Speciation of Fe in ground water using preconcentration on 3M Empore chelating disk and photometric reaction with ammonium thiocyanate	[35]
			Photometric determination of Cr (VI) using complexation with 1,5-diphenylcarbazide (DPC) and preconcentration on sulphonated PS-DVB resin	[36]
FIA flow-through cuvette insert	Polyurethane/ polyester	FDM	Insert into cuvette with two optical paths (2 and 10 mm) for photometric and fluorescent detection of bromthymol blue and fluorescein dyes	[37]
Gel electrophoresis tank and elution chamber	PLA/ABS n/a	FDM STL	ICP-MS detection of metalloproteins in rat plasma after gel electrophoresis	[38]
Micro free-flow electropho- resis device	ABS	FDM	Separation of fluorescent dyes with minimal surface adsorption	[39]
Stirring cage for SPE with housing for fibres and mag- netic stirring bar	PP	FDM	SPE of eight bisphenols (A, AF,AP, C, BP, G, M and Z) from river waters using polycaprolactone microfibers followed by HPLC with spectrophotometric detection	[40]
Serpentine separation channel for isotachophoresis		DLP	Separation of anionic dyes	[41]

PMMA – poly(methyl methacrylate), PMA – polymethacrylate, PA – polyacrylate.

consuming glass milling or etching techniques. Another opportunity in production of flow cell was demonstrated by 3D printing with VeroClear-RGD810 resin. The printed polyacrylate material is optically transparent above 400 nm as shown in Fig. 4c. This range overlaps entirely the light emission spectrum of 380-600 nm of the most popular chemiluminescence reaction between luminol and hydrogen peroxide. Both conventional spiral type (Fig. 5b) and new advanced radial flow configuration (Fig. 5a) flow cells were printed and compared for detection hydrogen peroxide. The less tortuous radial flow-cell design provides a higher chemiluminescence response in terms of both the magnitude and the duration. It should be also noted that the production of spiral flow cells requires a substantial, up to 360 h, time for removal of support material from long internal channels after 3D printing, while same operation takes only 10 h for printed radial flow cell.

Another current trend includes the use of multi material printing, which offers expanded possibilities for a more efficient use of combination of physicochemical properties in one printed object and construction of multi-functional devices. Various materials including optically transparent (e. g. polyacrylate resin VeroClear, Stratasys), electrically conductive (Proto-pasta conductive PLA, Protoplant), thermally conductive (nylon

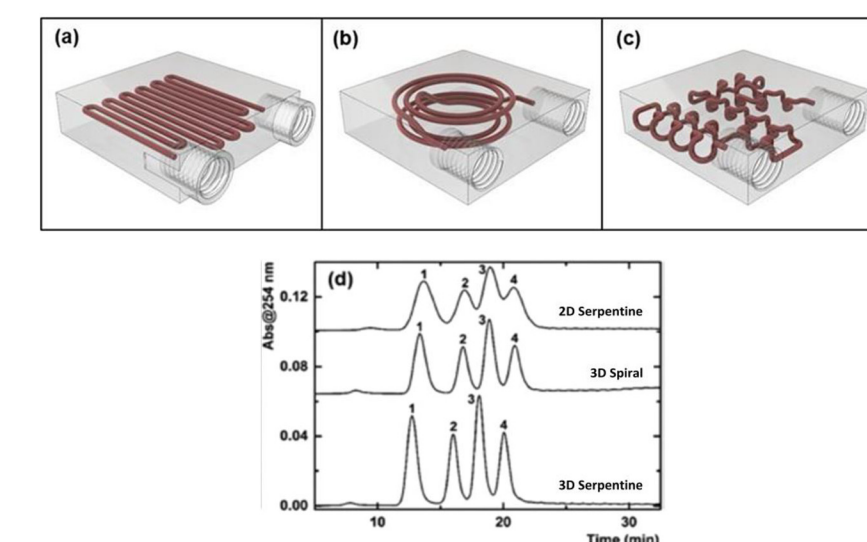


Fig. 4: 2D spiral (a), 3D spiral (b) and 3D serpentine (c) configurations of titanium alloy printed columns for HPLC and their comparative performance. Adapted from [12].

plastic Ice9™ rigid, TCPoly), porous (Poro-Lay Lay-Felt, MatterHackers) filaments are now commercially available that results in making more sophisticated devices by multi material printing. A good example of multi-functional operation of two materials with different physico-chemical properties within 3D printed microfluidic reactor has been recently reported [45]. The heating element was printed using graphene-PLA based filament and provided localised heating up to 120 °C by passing electric current. An electrically insulating and thermally conductive layer of microdiamond-ABS polymer composite printed on a top of heating element provided fast and uniform heating of the serpentine microfluidic reactor.

Actually, many of filaments with required physico-chemical properties can be prepared under laboratory conditions by composing common resins and micro- or nano- particles. Both thermal and electric conductivity of build material can be improved by addition of carbonaceous particles including microdiamond [13] having extremely high thermal conductivity [55], carbon black [56], carbon nanotubes [57] and grapheme [58] to base polymer. Magnetic induction can be attuned by addition of magnetite nanoparticles [53]. The most critical factor in preparation of high quality composites is homogeneous distribution of particles in 3D printed build material. Especially it is important for graphene nanoplatelets and carbon nanotubes. The distribution of nanoparticles estimated as the percolation threshold of nanoparticles depends on their geometrical shape, interaction between them and properties of base polymers. Often, the addition of certain components improving percolation of nanoparticles is required and resulted in development of so-called hybrid composite materials for 3D printing [59]. Undoubtedly the development of new hybrid composite materials is of great importance for the future of additive technologies.

Level 4: 3D printed devices with a significant role of chemical properties of build materials

The highest level of complexity for 3D printed devices used in analytical chemistry includes objects with a significant role of chemical interactions between analytes and surface of build material. Obviously, in this case a combination of various chemical interactions defines selectivity and sensitivity of the relevant analytical methods. These interactions and combinations of them can be effectively used for preconcentration and separation of analytes, enh ancement of analytical response or selective detection of chemical species.

Preconcentration

There are few reports on direct use of 3D printed passive samplers and extractors for preconcentration of analytes. It was found that the surface of 3D printed polyacrylate material has a substantial concentration of

Table 3: Analytical applications of 3D printed devices exploring specific physico-chemical properties of build material.

Physicochemical	Printing		Applications	Ref.	
property	Material Mode				
Optical transparency	PA/ABS	MJ/FDM	Radial flow cell for chemiluminescent detection of hydrogen peroxide in coffee	[10]	
, ,	PLA/PMMA	FDM	Microfluidic PLA based chip with PMMA optical transparent window for determination of NO_2^- , NO, total proteins and microorganism visualization	[46]	
	PLA	FDM	Flow cells for FIA-spectrophotometric determination of NO ₂ ⁻ via Griess reaction	[47]	
Electric conductivity	PLA-carbon black	FDM	Solvent sensor with sensitivity in the order of dichloromethane > chloroform > tetrahydrofuran > acetone > ethyl acetate > ethanol	[48]	
Thermal stability	SS 316/BN	BJ	Preconcentrator and injector for GC of volatile analytes and for gas sensing	[49]	
Thermal conductivity	PA	MJ	Liquid cooling assembly based on two Peltier elements for a deep-UV-LED optical detector for capillary HPLC	[50]	
	Titanium alloy (Ti6Al4V)	SLM	Compact flat HPLC columns with improved thermal exchange with Peltier elements	[51, 52]	
	Titanium alloy (Ti6Al4V)	SLM	Heating/cooling jacket of HPLC column with two recirculating zones and thermocouple fittings	[52]	
Thermal conductivity combined with electric insulation	ABS-microdiamond composite	FDM	Heater coating for spectrophotometric detection of NH_4^+ using reaction Berthelot	[45]	
Thermal conductivity combined with electric resistance	PLA-graphene composite	FDM	Joule type heater for spectrophotometric detection of $\mathrm{NH_4}^+$ using reaction Berthelot	[45]	
Magnetic induction	ABS containing magnetite nanoparticles	FDM	Flow sensor	[53]	
Elevated me- chanical strengths	Titanium alloy (Ti6Al4V)	SLM	Chromatographic columns	[54]	

SS - stainless steel, BN - boron nitride.

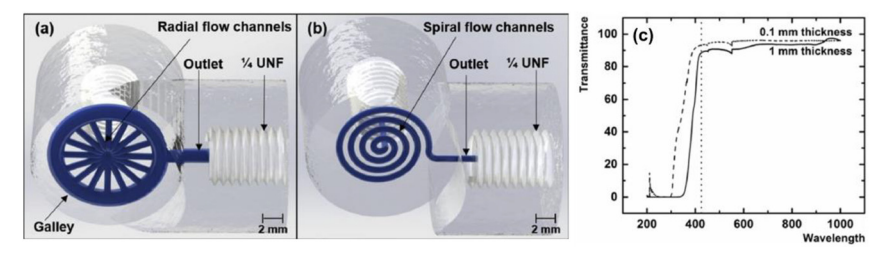


Fig. 5: 3D printed flow-cells for chemiluminescence detection (a - radial, b -spiral) and optical transmittance (c) of polyacrylate VeroClear-RGD810 resin.

carboxylic groups, which can be used for selective extraction of Mn, Ni, Zn, Cu, Cd, and Pb from seawater [60] for speciation analysis of iron [61] with ICP-MS detection. The structure of polyacrylate 3D printed microcuboid extractor and adsorption of metal ions as a function of pH are shown in Fig. 6. A filament LAY-FOMM-6 composed of rubber elastomer and PVA was used for 3D printing of porous inlays to Eppendorf tubes, which were used for extraction of drugs from waters without additional modification of polymer

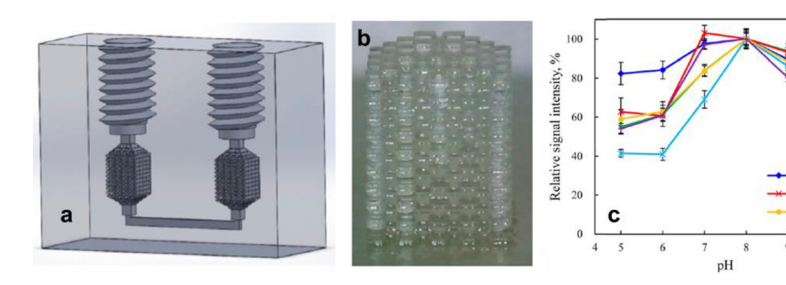


Fig. 6: Model of extractor (a). polyacrylate 3D printed device (b) and dependence of metal extraction as a function of pH (c). Adapted from [60].

surface [62]. Direct use of 3D printed porous material for collection of spilt oil was also reported in works [63, 64]. In this case efficiency of extraction was evaluated by intensity of fluorescence of polaromatic hydrocarbons (PAH). There is no information on properties of build polymer but it supposed to be hydrophobic interactions between printed porous collectors and neutral analytes, which are responsible for efficient extraction.

The selectivity and adsorption capacity of 3D printed polymer adsorber can be improved by direct chemical modification of surface functional groups or by coating with a layer of selective reagent. A covalent attachment of organic reagent to build material is relatively simple for acrylonitrile butadiene styrene (ABS) printed materials having nitrile reactive groups, for carboxyls on PA, hydroxyls on PVA and ester groups in PLA polymers [15]. A selective preconcentrator of Mercury was obtained by modification of 3D-printed cuboids with dithizone [65]. For this purpose, terminal methacrylate groups on the surface of printed PMMA cuboid or disk concentrator were converted into amino- groups by amidation reaction with 1,6-diaminohexane. Then prepared substrate reacted with dicarboxylate 1,5-diphenyl-3-thiocarbazone in presence of N-(3-dimethylaminopropyl)-N'-ethylcarbodiimide (EDC) to produce dithizone type structures. This preconcentrated Mercury on prepared device was determined by atomic absorption spectrophotometry.

The coating of PMA printed cuboid structure with TetraValent Actinides (TEVA) or Aliqat-336 reagents was used for selective SPE preconcentration and determination of U(VI) [66, 67]. Both reagents are hydrophobic trialkylmethylammonium chloride (or nitrate) salts, where alkyl is either octyl- or decyl- groups and retained by polymer via hydrophobic interactions.

One more possibility for modification of analytical capabilities of 3D printed devices is printing of bulk materials with embedded micro- or nanoparticles by using mixture of resin and suitable filler for production of preconcentrators. A highly selective Mercury scavenger in a form of filtering disk was prepared by SLS of polyamide-12 powder (~50 mm diameter) mixed with either 5 or 10 wt% of 3-mercaptopropylsilica (40–63 mm) [68]. The preconcentrated Mercury was eluted by thiourea solutions and detected by ICP-MS. The developed method was used for analysis of tap, lake, pond and river waters. TiO2 nanoparticles incorporated into PA based 3D printed microcuboid extractor were used selective isolation and ICP-MS determination of As(III), As(V), Se(IV) and Se(VI) species [69].

A significant drawback of 3D printed extractors is connected with low specific surface area, which resulted in low adsorption capacity of devices, especially in microfluidic formate. The use of metal-organic frameworks (MOF) having extremely high specific surface area for coating of printed structures could be a possible solution of this problem. As a proof of concept the application of submicrometric crystals of an imidazolate framework (ZIF-67)/polymer dispersion in organic solvent as mixed matrix coating (MMC) for 3D printed devices has been recently reported [66] without any analytical application. A step-by-step in-situ growth of porous Cu-BTC (BTC - benzenetricarboxylic acid) was also reported for coating on ABS printed framework. In this case the formation of 200-900 nm Cu-BTC nanoparticles on ABS was observed. The prepared adsorbent was used for quantitative removal of methylene blue dye from aqueous solutions. The maximum adsorption capacity was 63.3 mg of methylene blue dye per gram of MOF in printed structures. The quatitative adsorption of methylene blue was also observed for 3D printed MOF composed of Cu-BTC with calcium alginate and gelatine as biocompatible binders [84].

Separation

The reported examples of using 3D printed devices for separation of mixtures consider either discrimination of analytes on size in printed porous membranes [70, 71] or difference in adsorption energy of analytes onto surface of TLC plates having layers of polymer [74] or porous silica [73, 75]. Clearly, the structure of porous membranes is designed to prevent the diffusion of bulky components of blood and large biomolecules in to simplify biochemical analysis. Propeties of TLC plates with printed thin or ultra-thin layer of silica are similar to conventional plates, where porous layers are formed by other techniques. An interesting microstructures of 3D printed layer have been obtained in recent work [74] with separation of two proteins as a proof of concept. However, low surface area of printed layer limits loading capacity of TLC plates and adsorption properties of polyacrylate polymer are not properly characterised.

Until now no separations on 3D printed chromatographic columns have been reported in the literature. However, the interesting application of 3D printed porous filter with thickness of 5 mm composed of polyamide-12 with 5–10 wt% of 3-mercaptopropylsilica particles for dynamic preconcentration of Mercury followed by elution with thiourea solutions may be considered as analogue of a short chromatographic column [68].

Detection

Another promising area for application of 3D printed devices is production of chemical reactors for enhancement of analytical response and improving accuracy and versatility of linked detectors. Practically all of these reactors explore catalytic reaction on the surface of printed materials that removes limitation associated with low specific surface area of printed reactors. Obviously, a very small amounts of loaded catalysts is sufficient to accomplish catalytic conversion of analytes into more suitable for detection form.

Three interesting catalytic conversion reactions on metal printing devices are proposed for post column gas phase hydrogenolysis of aldehydes to alkanes [76], conversion of carbon oxides into methane [79] and two stage transformation of organic compounds into methane [77, 78]. In the latter case, microreactor oxidizes carbon compounds to carbon dioxide and subsequently converts them to proportional amount of methane by methanation. This technology provides carbon compound independent response that improves sensitivity, accuracy and precision of Flame Ionisation Detector (FID). It should be noted that above described devices known as jetanizer™, metanizer™ and catalytic process Polyarc® developed by Activated Research Company (Eden Prairie, MN, USA) represent the examples of the most successful commercialization of 3D printing technologies in analytical chemistry.

The catalytic activity of enzymes immobilised on the surface of polymer or metal oxide nanoparticles mimicking enzyme activity was used in 3D printed reactors for sensitive and selective determination of glucose and lactate in various clinical samples (see Table 4). The covalent attachment of enzymes can be performed via initial activation of the surface of ABS printed cuboid reactor (see Fig. 6b) with glutaraldehyde [83]. Chemical modification of printed PLA surface with piranha solution, peracetic acid, and a silane coupling agent was suggested for the preparation of activated matrix with reactive functional groups for immobilisation of various enzymes [85]. The obvious drawbacks of enzyme containing 3D printed reactors is a relatively low specific surface area (e.g. 2.2 m²/g as noted in work [85]) and a limited stability of immobilised enzymes. From this point of view, the application of catalytic reactors with embedded metal oxide nanoparticles (CuO [82], Fe₂O₃ [81] and Fe₃O₄ [80, 81]), which can mimick enzyme activity, looks very promising for detection of biomolecules.

Electrochemical reactions

Technically electrochemical detection should be considered apart the section Detection as it includes different electrochemical reactions at the surface of 3D printed electrodes. The development of 3D printed

Table 4: Analytical applications of 3D printed devices using specific interaction of analytes with build material.

-		Device and its analytical application	Refs.
Material	Mode		
PA	SLA	Microcuboid extractor with carboxylic groups at the surface of build material for SPE of metal ions from seawater	[60]
		Microcuboid extractor with carboxylic groups at the surface of build material for speciation of iron in natural waters	[61]
РМА	SLA	Preconcentration of U(VI) on microcuboid extractor coated with Aliquat-336 or TEVA followed by ICP-MS determination	[66, 67]
РММА	SLA	3D-printed cuboid extractor with grafted dithizone reagent for preconcentration and determination of Hg by AAS	[65]
Polyamide-12 - 5-10% 3-mercaptopropylsilica	SLS	Chelating disks (5 \times 16.5 mm diameter) for selective preconcentration of Hg and determination in natural	[68]
DA marsin with 40/ TiO	CLA	waters by ICP-MS	[40]
=	SLA		[69]
PLA/Lay Felt	FDM	SPE extraction of PAH from spilt oil on printed porous adsorbent followed by fluorescent detection	[63, 64]
LAY-FOMM 60	FDM	Porous polymer inlays in Eppendorf tubes for SPE extraction of glimepiride	[62]
PLA/Lay-Felt	FDM	Passive sampler for preconcentration of atrazine and nitrate on hypercrosslinked polystyrene	[70]
Conductive PLA/Lay Felt	FDM	Preconcentration of Cl $^-$, NO $_3$ $^-$, ClO $_4$ $^-$ and SO $_4$ 2 -, F- and HPO $_4$ 2 -, analysis of soil	[71]
Silica particles slurry	FDM	Separation of 6 lipophilic organic dyes	[73]
PA Silica particles slurry	MJ FDM	Separation of organic dyes, proteins HPTLC combined with 1H NMR spectroscopy of model	[74] [75]
		analytes	
Steel with catalyst	SLM	Post-column catalytic hydrogenolysis of aldehydes to alkanes to improve sensitivity of FID	[76]
Steel with catalyst (Ce, Co)	SLM	Two stage post column conversion of organic com- pounds for more accurate and sensitive FID detection	[77, 78]
Steel with catalyst	SLM	Conversion of CO and CO ₂ to methane to improve sensitivity of FID detection	[79]
ABS/Fe ₃ O ₄ and PVA/o- phenylenediamine	FDM	Catalytic/photometric determination of glucose in clinical samples	[80]
PLA/Fe ₂ O ₃ /Fe ₃ O ₄	FDM	Catalytic/photometric determination of glucose in clin-	[81]
•	ED	ical samples with 3,3′,5,5′-tetramethylbenzidine	[06]
•		ical samples with 2',7'-dichlorodihydrofluorescein	[82]
ABS	FDM		[83]
PLA/ABS with carbon filler	FDM	Three electrode cell for differential pulse voltametric	[72]
	PMA PMMA Polyamide-12 - 5-10% 3-mercaptopropylsilica PA resin with 1% TiO ₂ nanoparticles PLA/Lay Felt LAY-FOMM 60 PLA/Lay-Felt Conductive PLA/Lay Felt Silica particles slurry PA Silica particles slurry Steel with catalyst Steel with catalyst (Ce, Co) Steel with catalyst ABS/Fe ₃ O ₄ and PVA/o-phenylenediamine PLA/Fe ₂ O ₃ /Fe ₃ O ₄ nanoparticles PLA/CuO nanoparticles ABS PLA/ABS with carbon	PMA SLA PMMA SLA Polyamide-12 - 5-10% 3-mercaptopropylsilica PA resin with 1% TiO2 1AAA SLA PLA/Lay Felt FDM LAY-FOMM 60 FDM PLA/Lay-Felt FDM Conductive PLA/Lay Felt FDM Silica particles slurry FDM Silica particles slurry FDM Silica particles slurry FDM Silica particles slurry FDM Silica particles slurry FDM Silica particles slurry FDM ABS/Fe3O4 and PVA/o-phenylenediamine PLA/Fe2O3/Fe3O4 FDM ABS/Fe3O4 FDM ABS FDM PLA/ABS with carbon FDM	PA SLA Microcuboid extractor with carboxylic groups at the surface of build material for SPE of metal ions from seawater Microcuboid extractor with carboxylic groups at the surface of build material for SPE of metal ions from seawater Microcuboid extractor with carboxylic groups at the surface of build material for speciation of iron in natural waters PMA SLA Preconcentration of U(VI) on microcuboid extractor coated with Aliquat-336 or TEVA followed by ICP-MS determination PMMA SLA 3D-printed cuboid extractor with grafted dithizone reagent for preconcentration and determination of Hg by AAS Polyamide-12 – 5–10% SLS Chelating disks (5 × 16.5 mm diameter) for selective preconcentration of Hg and determination in natural waters by ICP-MS PA resin with 1% TiO ₂ SLA PA printed holder with PA/TiO ₂ cuboid adsorption unit for speciation of As and Se by ICP-MS PLA/Lay Felt FDM SPE extraction of PAH from spilt oil on printed porous adsorbent followed by fluorescent detection LAY-FOMM 60 FDM Porous polymer inlays in Eppendorf tubes for SPE extraction of glimepiride PLA/Lay-Felt FDM Passive sampler for preconcentration of atrazine and nitrate on hypercrosslinked polystyrene Conductive PLA/Lay Felt FDM Preconcentration of Cl-, NO ₃ -, ClO ₄ - and SO ₄ ² -, F- and HPO ₄ ² -, analysis of soil Silica particles slurry FDM Separation of 6 lipophilic organic dyes Separation of 6 lipophilic organic dyes Steel with catalyst SLM Separation of of granic dyes, proteins SILICa particles slurry FDM Separation of of Opanic dyes, proteins SILICa particles slurry FDM Separation of of Opanic dyes, proteins SILICa particles slurry FDM Separation of of Upophilic organic dyes Separation of of passic dyes, proteins SILICa particles slurry FDM Separation of of Opanic dyes, proteins SILICa particles slurry FDM Separation of of Opanic dyes, proteins SILICa particles slurry FDM Separation of of Opanic dyes, proteins SILICa particles slurry FDM Catalytic/photometric determination of gluco

electrodes and electrochemical sensors, especially in microfludics, is a huge and a separate area of analytical chemistry. In many cases printed electrodes can be considered as conducting coatings or 2D printed objects. There are few recently published reviews considering this specific area of research [5, 6, 8, 86–88], so this topic is not discussed in the current review.

Conclusions

This review analysed current trends in the development of 3D printed devices and their application in analytical chemistry. A new classification of 3D printed devices based on their complexity and operational multi-functionality is suggested. Four levels of complexity and functionality are outlined and briefly described with some representative examples for practical applications. Clearly, the design of new and improvement of existing composite materials with required physico-chemical properties, a more extensive use of reactive and functional materials, multimaterial printing represent future tasks in development of 3D printed devices for analytical applications. A possibility of combining new selective and efficient heterophase reactions in one printed unit is of great interest too.

References

- [1] V. Gupta, P. N. Nesterenko, B. Paull. 3D Printing in Chemical Sciences: Applications across Chemistry. RSC, Cambridge (2019).
- [2] B. Gross, S. Y. Lockwood, D. M. Spence. Anal. Chem. 89, 57 (2017).
- [3] U. Kalsoom, P. N. Nesterenko, B. Paull. Trac. Trends Anal. Chem. 105, 492 (2018).
- [4] D. J. Cocovi-Solberg, P. J. Worsfold, M. Miro. Trac. Trends Anal. Chem. 108, 13 (2018).
- [5] Y. Ni, R. Ji, K. Long, T. Bu, K. Chen, S. Zhuang. Appl. Spectrosc. Rev. 52, 623 (2017).
- [6] T. Han, S. Kundu, A. Nag, Y. Xu. Sensors (Switzerland) 19, 1706 (2019).
- [7] A. Lambert, S. Valiulis, Q. Cheng. ACS Sens. 3, 2475 (2018).
- [8] C. L. Manzanares Palenzuela, M. Pumera. Trac. Trends Anal. Chem. 103, 110 (2018).
- [9] J. F. Rusling. ACS Sens. 3, 522 (2018).
- [10] V. Gupta, P. Mahbub, P. N. Nesterenko, B. Paull, Anal. Chim. Acta 1005, 81 (2018).
- [11] T. W. Monaghan, M. J. Harding, S. D. R. Christie, R. J. Friel. Plos One 14, e0224492 (2019).
- [12] V. Gupta, S. Beirne, P. N. Nesterenko, B. Paull. Anal. Chem. 90, 1186 (2018).
- [13] U. Kalsoom, A. Peristyy, P. N. Nesterenko, B. Paull. RSC Adv. 6, 38140 (2016).
- [14] N. P. Macdonald, J. M. Cabot, P. Smejkal, R. M. Guijt, B. Paull, M. C. Breadmore. Anal. Chem. 89, 3858 (2017).
- [15] M. R. Hartings, Z. Ahmed. Nat. Rev. Chem. 3, 305 (2019).
- [16] S. Rossi, A. Puglisi, M. Benaglia. Chem. Cat. Chem. 10, 1512 (2018).
- [17] E. G. Gordeev, E. S. Degtyareva, V. P. Ananikov. Russ. Chem. Bull. 65, 1637 (2016).
- [18] C. Hurt, M. Brandt, S. S. Priya, T. Bhatelia, J. Patel, P. R. Selvakannan, S. Bhargava. Catal. Sci. Technol. 7, 3421 (2017).
- [19] C. Parra-Cabrera, C. Achille, S. Kuhn, R. Ameloot. Chem. Soc. Rev. 47, 209 (2018).
- [20] X. Zhou, C. Liu. Adv. Funct. Mater. 27, 1701134 (2017).
- [21] A. K. Au, W. Huynh, L. F. Horowitz, A. Folch. Angew. Chem. Int. Ed. 55, 3862 (2016).
- [22] A. Ambrosi, M. Pumera. Chem. Soc. Rev. 45, 2740 (2016).
- [23] T. Baden, A. M. Chagas, G. J. Gage, T. C. Marzullo, L. L. Prieto-Godino, T. Euler. PLOS Biol. 13, e1002175 (2015).
- [24] F. Cecil, M. Zhang, R. M. Guijt, A. Henderson, P. N. Nesterenko, B. Paull, M. C. Breadmore, M. Macka. Anal. Chim. Acta 965, 131
- [25] L. D. Casto, K. B. Do, C. A. Baker. Anal. Chem. 91, 9451 (2019).
- [26] J. Prikryl, F. Foret. Anal. Chem. 86, 11951 (2014).
- [27] K. J. M. Francisco, C. L. do Lago. *Talanta* **185**, 37 (2018).
- [28] K. S. Erokhin, E. G. Gordeev, V. P. Ananikov. Sci. Rep. 9, 20177 (2019).
- [29] C. K. Su, S. C. Hsia, Y. C. Sun. Anal. Chim. Acta 838, 58 (2014).
- [30] C. K. Su, M. H. Hsieh, Y. C. Sun. Anal. Chim. Acta 914, 110 (2016).
- [31] D. F. Thompson. J. Anal. Atomic Spectrom. 29, 2262 (2014).
- [32] S. Nawada, S. Dimartino, C. Fee. Chem. Eng. Sci. 164, 90 (2017).
- [33] E. Mattio, F. Robert-Peillard, C. Branger, K. Puzio, A. Margaillan, C. Brach-Papa, J. Knoery, J. L. Boudenne, B. Coulomb. Talanta **168,** 298 (2017).
- [34] E. Mattio, F. Robert-Peillard, L. Vassalo, C. Branger, A. Margaillan, C. Brach-Papa, J. Knoery, J. L. Boudenne, B. Coulomb. Talanta 183, 201 (2018).
- [35] C. Calderilla, F. Maya, V. Cerdá, L. O. Leal. Talanta 175, 463 (2017).
- [36] C. Calderilla, F. Maya, V. Cerdá, L. O. Leal. Talanta 184, 15 (2018).
- [37] M. Michalec, L. Tymecki. *Talanta* 190, 423 (2018).
- [38] D. Wang, B. He, X. Yan, Q. Nong, C. Wang, J. Jiang, L. Hu, G. Jiang. Talanta 197, 145 (2019).
- [39] S. K. Anciaux, M. T. Bowser. *Electrophoresis* **41,** 225 (2019).

- [40] I. H. Šrámková, B. Horstkotte, J. Erben, J. Chvojka, F. Švec, P. Solich, D. Satinsky. Anal. Chem. 92, 3964 (2020).
- [41] A. I. Shallan, P. Smejkal, M. Corban, R. M. Guijt, M. C. Breadmore. Anal. Chem. 86, 3124 (2014).
- [42] E. P. Nesterenko, P. N. Nesterenko, D. Connolly, F. Lacroix, B. Paull. J. Chromatogr. A. 1217, 2138 (2010).
- [43] C. Fee, S. Nawada, S. Dimartino. J. Chromatogr. A 1333, 18 (2014).
- [44] C. Salmean, S. Dimartino. Chromatographia 82, 443 (2019).
- [45] E. Fornells, E. Murray, S. Waheed, A. Morrin, D. Diamon, B. Paull, M. C. Breadmore. Anal. Chim. Acta 1098, 94 (2020).
- [46] L. P. Bressan, C. B. Adamo, R. F. Quero, D. P. De Jesus, J. A. F. Da Silva. Anal. Meth. 11, 1014 (2019).
- [47] Y. Liang, Q. Liu, S. Liu, X. Li, Y. Li, M. Zhang. Talanta 201, 460 (2019).
- [48] T. Sathies, P. Senthil, C. Prakash. Mater. Res. Expr. 6, 115349 (2019).
- [49] X. Huang, T. Bauder, T. Do, H. Suen, C. Boss, P. Kwon, J. Yeom. Sensors (Switzerland) 19, 2748 (2019).
- [50] S. C. Lam, V. Gupta, P. R. Haddad, B. Paull. Anal. Chem. 91, 8795 (2019).
- [51] V. Gupta, M. Talebi, J. Deverell, S. Sandron, P. N. Nesterenko, B. Heery, F. Thompson, S. Beirne, G. G. Wallace, B. Paull. *Anal. Chim. Acta* 910, 84 (2016).
- [52] M. Passamonti, I. L. Bremer, S. H. Nawada, S. A. Currivan, A. F. G. Gargano, P. J. Schoenmakers. Anal. Chem. 92, 2589 (2020).
- [53] S. J. Leigh, C. P. Purssell, D. R. Billson, D. A. Hutchins. Smart Mater. Struct. 23, 095039 (2014).
- [54] S. Sandron, B. Heery, V. Gupta, D. A. Collins, E. P. Nesterenko, P. N. Nesterenko, M. Talebi, S. Beirne, F. Thompson, G. G. Wallace, F. Regan, B. Paull. Analyst 139, 6343 (2014).
- [55] P. N. Nesterenko, P. R. Haddad. Anal. Bioanal. Chem. 396, 205 (2010).
- [56] N. Jayanth, P. Senthil. Compos. Part B Eng. 159, 224 (2019).
- [57] S. Shi, Y. Chen, J. Jing, L. Yang. RSC Adv. 9, 29980 (2019).
- [58] H. Guo, R. Lv, S. Bai. Nano Mater. Sci. 1, 101 (2019).
- [59] V. B. Mohan, B. J. Krebs, D. Bhattacharyya. Mater. Today Commun. 17, 554 (2018).
- [60] C. K. Su, P. J. Peng, Y. C. Sun. Anal. Chem. 87, 6945 (2015).
- [61] C. K. Su, Y. T. Chen, Y. C. Sun. Microchem. J. 146, 835 (2019).
- [62] M. Belka, S. Ulenberg, T. Baczek. Anal. Chem. 89, 4373 (2017).
- [63] Y. Zhang, J. Xiang, Y. Wang, Z. Qiao, W. Wang. Sens. Actuators, B Chem. 296, 126603 (2019).
- [64] Y. Zhang, J. Xiang, Y. Wang, Z. Qiao, W. Wang. A 3D printed centrifugal microfluidic platform for solid-phase-extraction and fluorescent detection of spilled oil in water, SPIE or full name - The Society of Photo-Optical Instrumentation Engineers (SPIE), San Francisco; United States (2019).
- [65] E. Mattio, N. Ollivier, F. Robert-Peillard, R. Di Rocco, C. Branger, A. Margaillan, C. Brach-Papa, J. Knoery, D. Bonne, J. L. Boudenne, B. Coulomb. *Anal. Chim. Acta* **1082**, 78 (2019).
- [66] M. Rodas Ceballos, J. M. Estela, V. Cerdá, L. Ferrer. Talanta 202, 267 (2019).
- [67] M. Rodas Ceballos, F. Gonzalez Serra, J. M. Estela, V. Cerdá, L. Ferrer. Talanta 196, 510 (2019).
- [68] S. Kulomäki, E. Lahtinen, S. Perämäki, A. Väisänen. Anal. Chim. Acta 1092, 24 (2019).
- [69] C. K. Su, W. C. Chen. Microchimica Acta 185, 268 (2018).
- [70] U. Kalsoom, C. K. Hasan, L. Tedone, C. Desire, F. Li, M. C. Breadmore, P. N. Nesterenko, B. Paull. Anal. Chem. 90, 12081 (2018).
- [71] M. L. Tan, M. Zhang, F. Li, F. Maya, M. C. Breadmore. J. Chromatogr. A 1595, 215 (2019).
- [72] V. Katseli, A. Economou, C. Kokkinos. *Talanta* 208, 120388 (2020).
- [73] D. Fichou, G. E. Morlock. Anal. Chem. 89, 2116 (2017).
- [74] N. P. Macdonald, S. A. Currivan, L. Tedone, B. Paull. Anal. Chem. 89, 2457 (2017).
- [75] I. Yüce, M. Mayr, G. E. Morlock. Anal. Chim. Acta 1087, 131 (2019).
- [76] J. Luong, X. Yang, Y. Hua, P. Yang, R. Gras. Anal. Chem. 90, 13855 (2018).
- [77] J. Luong, Y. Hua, R. Gras, X. Yang, P. Yang. J. Chromatogr. A 1609, 460460 (2019).
- [78] Y. Hua, J. Luong, X. Yang, L. Sieben, P. Yang, R. Gras. Anal. Meth. 11, 276 (2019).
- [79] R. Gras, Y. Hua, J. Luong, P. Qiao, X. G. Yang, P. Yang. J. Sep. Sci. 42, 2826 (2019).
- [80] C. K. Su, J. C. Chen. Anal. Chim. Acta 1036, 133 (2018).
- [81] C. K. Su, J. C. Chen. Sens. Actuators B Chem. 247, 641 (2017).
- [82] C. K. Su, H. H. Tseng. Microchimica Acta 186, 404 (2019).
- [83] C. K. Su, S. C. Yen, T. W. Li, Y. C. Sun. Anal. Chem. 88, 6265 (2016).
- [84] R. Pei, L. Fan, F. Zhao, J. Xiao, Y. Yang, A. Lai, S. F. Zhou, G. Zhan. J. Hazard. Mat. 384, 121418 (2020).
- [85] J. Ye, T. Chu, J. Chu, B. Gao, B. He. ACS Sustain. Chemi. Eng. 7, 18048 (2019).
- [86] R. M. Cardoso, D. M. H. Mendonç a, W. P. Silva, M. N. T. Silva, E. Nossol, R. A. B. da Silva, E. M. Richter, R. A. A. Muñ oz. Anal. Chim. Acta 1033, 49 (2018).
- [87] S. R. Ahammed, B. H. Babu, S. P. Dheeraj, A. Y. Shiferaw. Int. J. Innov. Technol. Expl. Eng. 9, 2182 (2019).
- [88] S. He, S. Feng, A. Nag, N. Afsarimanesh, T. Han, S. C. Mukhopadhyay. Sensors 20, 703 (2020).